Modeling and Analyzing Impacts of Drifting Anisotropic Ionospheric Irregularities on Inclined Geosynchronous SAR

Dong, Xichao; Hu, Jiaqi; Hu, Cheng; Li, Yuanhao; Sun, Shiyu

DOI
10.1109/ACCESS.2019.2944192

Publication date
2019

Document Version
Final published version

Published in
IEEE Access

IEEE Access
Multidisciplinary | Rapid Review | Open Access Journal

Received August 30, 2019, accepted September 15, 2019, date of publication September 27, 2019, date of current version October 15, 2019.

Digital Object Identifier 10.1109/ACCESS.2019.2944192

Modeling and Analyzing Impacts of Drifting Anisotropic Ionospheric Irregularities on Inclined Geosynchronous SAR

XICHAO DONG[1], JIAQI HU[1], CHENG HU[1,2], (Senior Member, IEEE), YUANHAO LI[3], (Member, IEEE), AND SHIYU SUN[1]

[1]School of Information and Electronics, Beijing Institute of Technology, Beijing 100081, China
[2]Key Laboratory of Electronic and Information Technology in Satellite Navigation, Ministry of Education, Beijing Institute of Technology, Beijing 100081, China
[3]Department of Geoscience and Remote Sensing, Delft University of Technology, 2628 CN Delft, The Netherlands

Corresponding author: Cheng Hu (cchchb@bit.edu.cn)

This work was supported in part by the National Natural Science Foundation of China (NSFC), under Grant 61971039 and Grant 61960206009, in part by the Special Fund for Research on National Major Research Instruments, NSFC, under Grant 61827901 and Grant 31727901, and in part by the Young Elite Scientists Sponsorship Program by CAST under Grant 2017QNRC001.

ABSTRACT The sub-satellite track of geosynchronous synthetic aperture radar (GEO SAR) presents the figure ''8'' or ''O'', which causes the great changes of platform motion direction and the different projection of anisotropic irregularities along the line-of-sight (LOS) direction. Due to the almost equal angle velocity to that of Earth, the GEO SAR has smaller ionospheric penetration point (IPP) scanning velocity which is much smaller to the counterpart of the low earth orbit SAR (LEO SAR) while is comparable to the drifting velocity of irregularities, which will affect the effective azimuthal velocity. These facts lead to the consequence that the satellite signals from the GEO SAR would become more vulnerable when they are transmitted in the environment where the ionospheric scintillation occurs. However, few works are focused on these mentioned issues towards the GEO SAR system. In this paper, the impacts of ionospheric scintillation on GEO SAR imaging will be analyzed considering the anisotropy and drifting velocity of irregularities. The anisotropy and drifting velocity effects can both originate from the effect on power spectral density (PSD) of phase screen which is used to model the ionospheric scintillation effects. Based on the data from international geomagnetic reference field (IGRF) and satellite tool kit (STK), the GEO SAR imaging simulations for different GEO SAR orbital configurations and positions are carried out. The simulation results demonstrate that the anisotropy and the drifting velocity of irregularities will cause the changes of stripe direction and affect the quality of GEO SAR images.

INDEX TERMS Anisotropy, drifting velocity, geosynchronous synthetic aperture radar (GEO SAR), ionospheric scintillation.

I. INTRODUCTION

The ionospheric irregularities in the ionosphere will introduce the amplitude and phase fluctuations to the signals from the geosynchronous synthetic aperture radar (GEO SAR), i.e. ionospheric scintillation [1], which will introduce the light and dark stripes and defocusing on SAR images. The low frequency synthetic aperture radar (SAR) system such as L-band and P-band will be affected seriously by ionospheric scintillation, and the light and dark stripes on SAR images have been observed in low earth orbit SAR (LEO SAR) [2]. The phase screen (PS) theory is a popular method to analyze the effect of ionospheric scintillation and lots of researches were carried out on the L-band and P-band LEO SAR imaging using PS theory [2], [3]. Meyer et al. made quantitative analyses of ionospheric scintillation on SAR imaging using Advanced Land Observing Satellite (ALOS) Phased-Array type L-band SAR (PALSAR) data near the equator, concluding that the ionospheric scintillation will introduce the amplitude and phase fluctuations and cause imaging defocusing [4]. The irregularities will drift zonally driven by the geomagnetic field, which affects effective scales of observed

The associate editor coordinating the review of this manuscript and approving it for publication was Gerardo Di Martino.

irregularities and causes SAR images defocusing. Kim et al. analyzed the influences of the drifting equatorial irregularities in the F region on SAR imaging by the diffraction stripes, and proposed a method to estimate the height and drifting velocity of irregularities by the observation geometry [5]. Besides, the distortions introduced by ionospheric scintillation can be corrected by Faraday rotation estimates and the proposed methodology has been validated using simulated P-band spaceborne SAR data in accordance with the characteristics of BIOMASS satellite [6]–[8].

In general, the irregularities elongate along the geomagnetic field. The angle between the track direction of LEO SAR and geomagnetic field is approximately invariable within the synthetic aperture time (SAT), which indicates that the anisotropy of irregularities have few effects on LEO SAR during SAT. Besides, the ionospheric penetration point (IPP) scanning velocity of LEO SAR can be up to thousands of meters per second, which is larger than the drift velocity of irregularities (about hundreds of meters per second in low latitude area). Thus, the effective azimuthal velocity is independent on the IPP scanning velocity. However, compared to the LEO SAR, L-band inclined GEO SAR is more sensitive to anisotropy drifting ionospheric irregularities. The sub-satellite track of GEO SAR is figure "8" or "O" [9] and the direction of platform changes greatly during the observation time, which causes great effects of the anisotropic irregularities on GEO SAR imaging. Furthermore, the angular velocity of GEO SAR is equivalent to that of the Earth rotation, leading to the IPP scanning velocity of GEO SAR is comparable to the drift velocity of irregularities in some orbital positions. Both of two velocities will affect the effective azimuthal velocity. However, most of the researches of ionospheric scintillation based on LEO SAR system are concentrated on the observation and verification and few that about the modelling of effects of irregularities on GEO SAR system.

Currently, the performance analysis of ionospheric scintillation on GEO SAR was carried out based on the point spread function [10] and scintillation sampling model [11], along with some equivalent validation experiments based on global navigation satellite systems [12]. The high latitude anisotropic irregularity effects were analyzed based on the observations of ALOS PALSAR [13], [14]. However, these studies didn't consider the influences of anisotropy and drifting velocity of irregularities on GEO SAR imaging for area targets.

This paper studies the impacts of anisotropic and drifting irregularities on GEO SAR based on the modified power spectrum density (PSD). The outline of this paper is as follows. In section II, the PSD of phase screen is modified based on the anisotropy and drifting velocity of irregularities. The ionospheric transfer function (ITF) based on the PS theory and the influenced GEO SAR signal are proposed in section III. In section IV, area targets at different GEO SAR orbital positions of different configurations are simulated and compared with the LEO SAR results. The paper is concluded in section V.

II. THE MODIFIED POWER SPECTRAL DENSITY

The ionospheric scintillation status can be modeled as a thin phase screen, and the random phase introduced by the irregularities can be obtained by its PSD. With the influences of geomagnetic activity, the drifting ionospheric irregularities will be elongated along the geomagnetic field and will obviously show anisotropic characters. The different projection of anisotropic irregularities along the line-of-sight (LOS) direction can be introduced by the significant variations of the GEO SAR motion. Besides, due to the similarity between the IPP scanning velocity of GEO SAR and the drifting velocity of irregularities, the signal propagation process would become sensitive to the drifting velocity. Therefore, the PSD of random phase should be modified considering the anisotropy and drifting velocity of the irregularities.

A. GEOMETRY OF GEO SAR AND IONOSPHERIC IRREGULARITIES

The amplitude fluctuations caused by the anisotropy of ionospheric irregularities are shown as light-dark stripes on SAR images, whose direction depends on the geomagnetic field and the direction of satellite motion, that is, the direction of stripes is $\vec{u} \times (\vec{l} \times \vec{B})$ [4], where $\vec{u}$ is the "up" unit vector, $\vec{l}$ is the vector of radar line of sight, $\vec{B}$ is the vector of geomagnetic field. This direction relates to the heading of radar beam when the irregularities are projected on the SAR image.

Fig.1 shows the geometrical relationship of the geomagnetic field and GEO SAR. S_n points to geomagnetic north and the irregularities elongate along the geomagnetic field **B** whose projection on the horizontal plane is S_n. The latitude and longitude of IPPs are (ϑ, ζ), z_0 points to ground, **k** is the wave propagation direction, $\mathbf{k_P}$ is the beam projection on the horizontal plane, v_{sat} is the GEO SAR velocity in the horizontal plane which can be obtained by satellite tool kit (STK), ψ is the magnetic inclination, χ is the magnetic declination, θ is the incident angle, and all these angles are measured at (ϑ, ζ). φ is the magnetic heading of the radar beam and $\Delta = |\varphi + \pi/2|$ is the magnetic heading of the platform motion (assuming that right side of geomagnetic north is positive for left-looking GEO SAR), which represents

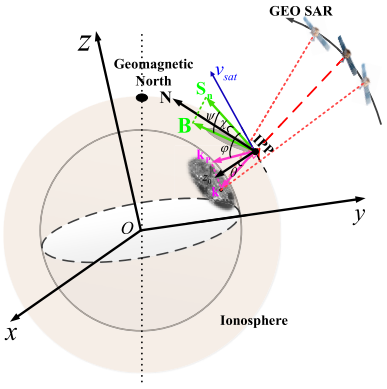

FIGURE 1. The geometrical relationship of the geomagnetic field and GEO SAR.

the angle between platform motion and geomagnetic field. The smaller $|\Delta - \pi|$ (when Δ is larger than $\pi/2$) or Δ (when Δ is smaller than $\pi/2$) leads to the more aligned of platform motion and geomagnetic field.

B. MODIFIED PSD AFFECTED BY ANISOTROPY

The PSD of phase screen can be expressed as Rino spectrum [2]:

$$S_{\phi 0}\left(\kappa_x, \kappa_y; \vartheta, \zeta\right) = \frac{\lambda^2 r_e^2 \sec^2\theta ab \left(2\pi/1000\right)^{p+1} C_k L}{\left[\kappa_0^2 + M\left(\vartheta,\zeta\right)\kappa_x^2 + N\left(\vartheta,\zeta\right)\kappa_x\kappa_y + P\left(\vartheta,\zeta\right)\kappa_y^2\right]^{(p+1)/2}} \tag{1}$$

where κ_x and κ_y are the wavenumbers in directions of geomagnetic north and east, r_e is the classic electron radius, $C_k L$ is the vertical integrated scintillation strength of 1 km scales, L_0 is the outer scale and p is the spectrum index. The coordinate transformation coefficients M, N and P depending on the directions of signal propagation and the geomagnetic field can convert the coordinate system where the irregularities are located to the SAR coordinate system for further analysis [15]:

$$\begin{aligned} M\left(\vartheta,\zeta\right) &= C_{11} + C_{33}\tan^2\theta\cos^2\varphi - 2C_{13}\tan\theta\cos\varphi \\ N\left(\vartheta,\zeta\right) &= 2\left[\begin{array}{l} C_{12} + C_{33}\tan^2\theta\sin\varphi\cos\varphi \\ -\tan\theta\left(C_{13}\sin\varphi + C_{23}\cos\varphi\right)\end{array}\right] \\ P\left(\vartheta,\zeta\right) &= C_{22} + C_{33}\tan^2\theta\sin^2\varphi - 2C_{23}\tan\theta\sin\varphi \end{aligned} \tag{2}$$

$$\begin{aligned} C_{11}\left(\vartheta,\zeta\right) &= a^2\cos^2\psi + \sin^2\psi\left(b^2\sin^2\delta + \cos^2\delta\right) \\ C_{22}\left(\vartheta,\zeta\right) &= b^2\cos^2\delta + \sin^2\delta \\ C_{33}\left(\vartheta,\zeta\right) &= a^2\sin^2\psi + \cos^2\psi\left(b^2\sin^2\delta + \cos^2\delta\right) \\ C_{12}\left(\vartheta,\zeta\right) &= C_{21} = \left(b^2 - 1\right)\sin\psi\sin\delta\cos\delta \\ C_{13}\left(\vartheta,\zeta\right) &= C_{31} = \left(a^2 - b^2\sin^2\delta - \cos^2\delta\right)\sin\psi\cos\psi \\ C_{23}\left(\vartheta,\zeta\right) &= C_{32} = -\left(b^2 - 1\right)\cos\psi\sin\delta\cos\delta \end{aligned} \tag{3}$$

where a and b are the scale factors which are along and perpendicular to the axis of ionospheric irregularities, respectively, and a:b is the anisotropy ratio.

The two-dimensional phase screen can be obtained from filtering the complex Gaussian random sequence by a filter which is constructed from PSD [16]:

$$\phi\left(x,y\right) = IDFT\left[\sqrt{S_{\phi 0}\left(\kappa_x,\kappa_y;\vartheta,\zeta\right)\cdot\left[\left(2\pi\right)^2/L_xL_y\right]} \cdot\sqrt{1/2}\left(g_{1m} + ig_{2m}\right)\right] \tag{4}$$

where L_x and L_y are the length and width of phase screen, and g_{im} is the independent complex Gaussian variable (0-mean, 1-variance).

Assuming that the PS extends along the geomagnetic north and east, the PS needs to be set the spacing to determine the wavenumber in the SAR coordinate system. The azimuth spacing ΔS_a and the range spacing ΔS_r of SAR image are:

$$\begin{aligned} \Delta S_a &= \frac{V_S}{PRF} \\ \Delta S_r &= \frac{c}{2f_s} \end{aligned} \tag{5}$$

where V_S is radar velocity relative to the ground, PRF is pulse repetition frequency, f_s is sampling frequency, and c is light speed. The ground sampling spacing is $\Delta S_{gr} = \Delta S_r/sin\left(\gamma\right)$ and γ is the incident angle. The geomagnetic north and east spacings of PS can be obtained from rotating the azimuth and the ground sampling spacings by $-\varphi$ [2], that is:

$$\begin{aligned} \Delta S_e &= \left|\Delta S_{gr}\sin\left(-\varphi\right) - \Delta S_a\cos\left(-\varphi\right) - v_{0e}/PRF\right| \\ \Delta S_n &= \left|\Delta S_{gr}\cos\left(-\varphi\right) + \Delta S_a\sin\left(-\varphi\right) - v_{0n}/PRF\right| \end{aligned} \tag{6}$$

where v_{0e} and v_{0n} are the geomagnetic east and north drifting velocity of the irregularities, respectively.

C. MODIFIED PSD AFFECTED BY THE DRIFT VELOCITY

Irregularities in low latitude have zonal drifting velocity with a typical value of around 100m/s [17]. The effects of drifting velocity on GEO SAR and LEO SAR are different. Fig.2 is the IPP scanning velocity in one day of GEO SAR and LEO SAR, where the parameters are from Table. 1. For LEO SAR, the drifting velocity is much smaller than the IPP scanning velocity which is up to several kilometers per second, as shown in Fig.2 (a). The effective velocity only depends on the IPP scanning velocity, and the effects of drifting velocity can be ignored for LEO SAR. However, the IPP scanning velocity of GEO SAR is at the same level as the irregularities drifting velocity as shown in Fig.2 (b), and the effective velocity will depend on the both of two velocities. Thus, the drifting velocity of irregularities needs to be considered for GEO SAR.

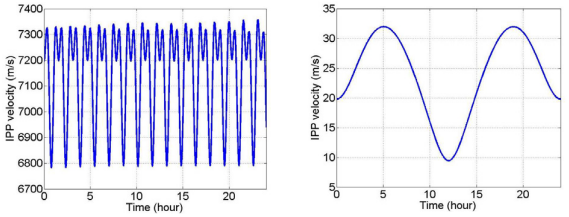

FIGURE 2. The IPP velocity of LEO SAR and GEO SAR (big figure "8" nadir track) with one day. The orbital parameters are from Table 1. (a) LEO SAR IPP velocity (b) GEO SAR IPP velocity

TABLE 1. Satellite parameters.

Orbital parameters	Big "8"	Small "8"	ALOS
Semimajor axis (km)	42164.17		1328.75
Inclination (°)	53	16	98.16
Longitude of ascending node (°)	113	88	-
Eccentricity	0	0	0

Assuming that $\vec{v}_0$ is the irregularity drifting velocity and points to geomagnetic east-west, which is constant within

the SAT under the assuming of "frozen field". Therefore, the random fluctuation $\xi(\vec{r}, t)$ of electron density satisfies:

$$\xi(\vec{r}, t_0 + t) = \xi(\vec{r} - \vec{v}_0 t, t_0) \tag{7}$$

and the autocorrelation function $B_\phi(\vec{r}, t)$ satisfies:

$$B_\phi(\vec{r}, t_0 + t) = B_\phi(\vec{r} - \vec{v}_0 t, t_0) \tag{8}$$

where $\vec{r}$ represents the spatial position and t represents the slow time. $B_\phi(\vec{r}, t)$ can be modified by drifting velocity as:

$$\begin{aligned} B_\phi(\vec{r}, t) &= B_{\phi 0}(\vec{r} - \vec{v}_0 t) = B_{\phi 0}\left(\vec{v}_i \frac{\vec{r}}{\vec{v}_i} - \vec{v}_0 \frac{\vec{r}}{\vec{v}_i}\right) \\ &= B_{\phi 0}\left(\frac{\vec{v}_{eff}}{\vec{v}_i}\vec{r}\right) = B_{\phi 0}(\beta \vec{r}) \end{aligned} \tag{9}$$

It can be found that the drifting velocity causes a scale change, where $\vec{v}_i$ is the IPP scanning velocity, $\vec{v}_{eff}$ is the relative velocity of IPP scanning velocity and drifting velocity, which represents the effective azimuthal velocity of GEO SAR. Assuming that irregularities drift along the latitude, the relative velocity $\vec{v}_{eff}$ can be expressed as [15]:

$$\begin{aligned} v_{eff} &= \sqrt{\frac{PV_{ex}^2 - NV_{ex}V_{ey} + MV_{ey}^2}{MP - N^2/4}} \\ V_{ex} &= -(V_{ix} - \tan\theta \cos\varphi V_{iz}) \\ V_{ey} &= v_0 - (V_{iy} - \tan\theta \sin\varphi V_{iz}) \end{aligned} \tag{10}$$

where V_{ix}, V_{iy}, and V_{iz} are the magnetic north, magnetic east, and vertical downward components of the IPP scanning velocity, respectively, and $\beta = v_{eff}/v_i$ is the velocity scale index. For LEO SAR, the IPP scanning velocity is much larger than the irregularities drifting velocity ($v_i \gg v_0$), that is, $v_{eff} \approx v_i$ and $\beta \approx 1$. Thus, the drifting velocity can be ignored for LEO SAR. At some orbital locations of GEO SAR, β will vary with the drifting velocity and will not be constant at 1, which will affect the PSD of the random phase.

According to the Wiener-Sinqin theorem, the phase autocorrelation function and its PSD are Fourier transform pair, i.e. $B_\phi^0(\vec{r}) \underset{S_\phi^0}{\longleftrightarrow} (\vec{\kappa})$. The modified PSD can be obtained by:

$$\begin{aligned} S_\phi(\vec{\kappa}) &= \frac{1}{\beta} S_{\phi 0}\left(\frac{\vec{\kappa}}{\beta}\right) \\ &= \beta^p \frac{\lambda^2 r_e^2 \sec^2\theta ab \left(2\pi/1000\right)^{p+1} C_k L}{\left(\beta^2 \kappa_0^2 + M\kappa_x^2 + N\kappa_x\kappa_y + P\kappa_y^2\right)^{(p+1)/2}} \end{aligned} \tag{11}$$

It can be indicated that when $|\beta|$ is larger, the cut-off frequency of PSD is larger and the coherent length is smaller, which will cause the stronger scintillation intensity on the SAR image.

III. GEO SAR SIGNAL INFLUENCED BY IRREGULARITIES

The ionospheric scintillation will introduce the amplitude and phase errors on GEO SAR signal, which can be expressed by ionospheric transfer function(ITF) [2]:

$$D_{ITF}(x) = IFFT\left\{\exp\left[i\frac{\kappa_x^2}{2k_0} z \sec\theta\right] FFT\left\{e^{i\phi(x)}\right\}\right\} \tag{12}$$

where z is the distance from phase screen to receiver, κ_x is the frequency of wavenumber domain which is the Fourier transform of azimuth position x, θ is the incident angle, $k_0 = 2\pi/\lambda$ is the wavenumber, and $\phi(x)$ is the random phase introduced by the irregularities, i.e. phase screen.

Due to the large imaging scene of GEO SAR, the irregularities generate different amplitude and phase fluctuations to the signal at different pulse repetition times (PRT). Besides, the ITFs at different IPP positions are also different for every synthetic aperture time (SAT), as shown in Fig.3. A, B, and C are IPPs which have different latitudes and longitudes of the target P for different SAT. Therefore, ITF can be expressed by the function of spatial sampling u, latitudes ϑ, and longitudes ζ, i.e. $D_{ITF}(u; \vartheta, \zeta)$.

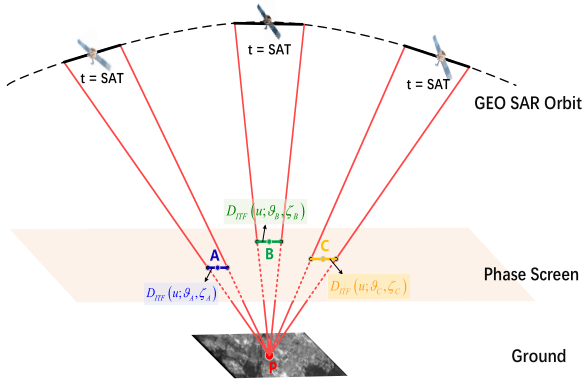

FIGURE 3. The ionospheric scintillation effects on GEO SAR signal propagation for different IPP positions and different SAT.

The ideal signal of GEO SAR can be written as:

$$s_0(t, u) = W_r\left(t - \frac{2R}{c}\right) W_a(y - u) P\left(t - \frac{2R}{c}\right) \tag{13}$$

where u is the spatial sampling in azimuth, P is the waveform of signal, W_r and W_a are the envelope functions of range and azimuthal direction, respectively. The propagation of the signal in the irregularities can be divided into two parts: the down-propagation from GEO SAR to the ground, and the up-propagation from ground back to GEO SAR.

Considering the IPP A, when the signal propagates from GEO SAR to the ground, the signal model in the presence of ionospheric scintillation can be written as:

$$s_{1r}(t, u) = \sigma_p s_0(t, u) \cdot D_{ITF}(u_p; \vartheta_A, \zeta_A) = \sigma_p' \cdot s_0(t, u) \tag{14}$$

where σ_p is the scattering coefficient of target p and (ϑ_A, ζ_A) is the latitudes and longitudes of IPP A. $\sigma_p' = \sigma_p s_0(t, u)$ represents that the scattering coefficients of every point targets in the imaging area are modulated by $D_{ITF}(u; \vartheta_A, \zeta_A)$ during observation time. It is noted that this method can get rid of the assumption of small scene assumption in LEO SAR [2].

When the signal propagates from the ground back to GEO SAR, the signal will be affected by ionospheric scintillation at different spatial positions, so the different amplitude and phase fluctuations are introduced in the aperture:

$$s_{2r}(t, u) = \sigma_p' \cdot s_0(t, u) \cdot D_{ITF2}(u; \vartheta_A, \zeta_A) \tag{15}$$

where $D_{ITF2}(u;\vartheta_A,\zeta_A)$ is the ITF introduced in the different spatial positions for IPP A.

Assuming that the irregularities are stationary random processes during the propagation time and their statistical properties do not vary with time, it can be considered that ITFs are equal when the signal propagates up and down [11], i.e.:

$$D_{down}(u;\vartheta_A,\zeta_A)=D_{up}(u;\vartheta_A,\zeta_A)=D_{ITF}(u;\vartheta_A,\zeta_A) \quad (16)$$

Then the area target echoes can be obtained by summing these of multiple point targets:

$$\begin{aligned} &s^{iono}(t,u)\\ &=\sum_p s_p(t,u)\\ &=D_{ITF}(u;\vartheta_A,\zeta_A)\sum_p \sigma_p\cdot D_{ITF}\left(u_p;\vartheta_A,\zeta_A\right)s_0(t,u) \end{aligned} \quad (17)$$

Therefore, the influences of ionospheric scintillation on GEO SAR signals can be expressed in two parts: 1) when the signal propagates from GEO SAR through ionosphere to the ground, the ITFs are directly modulated on the scattering coefficients of the ground targets, appearing the light-dark streaks on the SAR image; 2) when the signal returns to GEO SAR, the ITFs can be superimposed on signals at different spatial positions and affect the coherent accumulation of echoes.

IV. SIMULATIONS AND DISCUSSION

A. SIMULATING SCENE SELECTION

Due to the large imaging scene of GEO SAR, the IPP velocity, the geomagnetic field and the magnetic heading are different in different orbital positions. The ALOS configuration is also used to simulate the LEO SAR condition, which can be compared with the GEO SAR results. Firstly, in this section, we select 3 locations in 2 GEO SAR configurations and 1 location in LEO SAR configuration to analyze the effects of anisotropy and drifting velocity on imaging. The GEO SAR and LEO SAR configuration parameters and phase screen parameters are as in Table 1 and Table 2, respectively, where the height of ionosphere is set as 350km.

TABLE 2. Phase screen parameters.

Parameters	Value	Parameters	Value
Samples in azimuth	15001	C_kL	5×10^{34}
Samples in range	5000	p	3

The GEO SAR and ALOS sub-satellite tracks are in Fig.4, where three points are selected for each GEO SAR and the interval between two adjacent points is 600s. The IPP velocity of GEO SAR is much smaller than that of LEO SAR which is about 7km/s. The point of ALOS is selected above near the equator. The geographic north N and geomagnetic north S_n are marked in the figure.

Assuming that the drifting velocity of the irregularity is 100 m/s along the geomagnetic east, the geomagnetic field

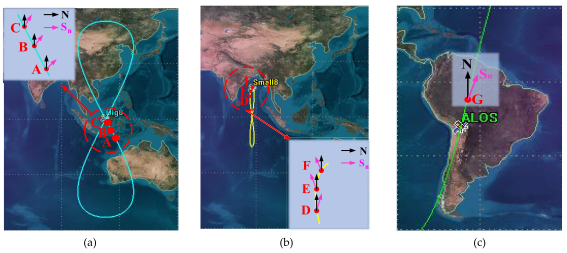

FIGURE 4. The sub-satellite tracks of GEO SAR and ALOS (a): Big "8" GEO SAR (b): Small "8" GEO SAR (c): ALOS PALSAR.

parameters φ, ψ, χ and θ at the IPP locations shown in Table 3 can be obtained from the International Geomagnetic Reference Field (IGRF) and the geometrical relationship in Fig.1. In the following, these parameters are used to simulate the phase screen and imaging process.

TABLE 3. Parameters of geometry for different satellite configurations.

		φ (°)	ψ (°)	χ (°)	θ (°)
Big "8"	A	2.21	-46.68	-4.99	88.26
	B	-2.63	-40.67	-4.35	92.26
	C	-7.05	-33.60	-3.82	96.24
Small "8"	D	44.38	34.50	0.88	103.60
	E	44.53	36.22	-2.92	103.48
	F	46.64	41.95	1.55	103.27
ALOS	G	83.50	14.40	-5.70	36.40

S_4 and σ_φ are used to evaluate the strength of scintillation generally, which are defined as:

$$\begin{aligned} S_4 &= \sqrt{\left(\langle A_{ITF}^2\rangle-\langle A_{ITF}\rangle^2\right)\Big/\langle A_{ITF}\rangle^2}\\ \sigma_\varphi &= \sqrt{\left(\langle P_{ITF}^2\rangle-\langle P_{ITF}\rangle^2\right)} \end{aligned} \quad (18)$$

where A_{ITF} and P_{ITF} are the amplitude and phase of ITF, respectively, and $\langle\cdot\rangle$ represents mathematical expectation. In general, S_4 and σ_φ reflects the strength of amplitude and phase scintillations.

B. SIMULATING RESULTS

The ionospheric fluctuations are generated based on the PS theory and imposed into the ideal SAR image. The whole results are shown in Fig.5, including the phase screen results, the ITF amplitude and phase fluctuations, the contaminated images by scintillation, the point target in center of the scene whose scattering coefficient is increased by 40dB before processing, and the azimuth envelope of the point target. The ionospheric scintillation will not affect the range imaging, so we only consider the azimuth. Besides, Δ can be calculated from Table 3 and β can be obtained from the satellite tool kit (STK) as shown in Table 4. S_4, σ_φ, and peak sidelobe radio (PSLR) of point target are also calculated as shown in Table 4.

From Table 4, it can be seen that the Δ or $|\Delta-\pi|$ of D, E, and F are smaller than A, B, and C, which means more aligned of platform motion and geomagnetic field. In this condition, the S_4 of D, E, and F are smaller than A, B, and C. Besides, the σ_φ and sidelobes of A, B, and C are higher than

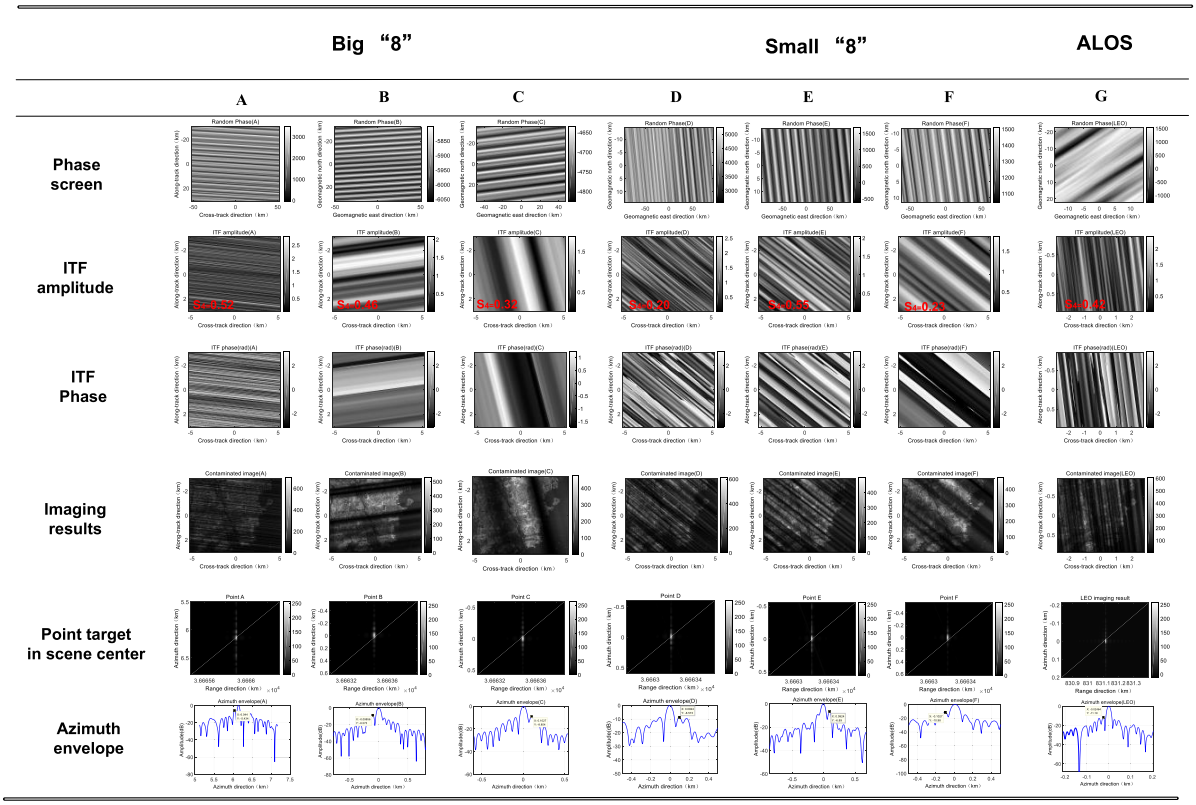

FIGURE 5. The simulating results at position A to F of GEO SAR and compared results of LEO SAR.

TABLE 4. Δ, β, S_4, σ_φ, and PSLR of GEO and LEO system.

		Δ (°)	β	S_4	σ_φ (rad)	PSLR(dB)
Big"8"	A	92.21	0.72	0.52	1.82	-5.43
	B	87.37	0.11	0.46	1.34	-8.57
	C	82.95	0.10	0.32	1.35	-8.85
Small" 8"	D	134.38	0.13	0.20	1.29	-8.57
	E	134.53	0.35	0.55	1.74	-6.89
	F	136.64	0.10	0.23	0.94	-10.96
ALOS	G	6.50	1.00	0.42	0.83	-11.19

D, E and F. These behaviors indicate that the more aligned of platform motion and geomagnetic field cause the weaker amplitude fluctuation and the better imaging quality.

From Fig.5 and Table 4, it can be seen that the larger β will cause the stronger scintillation intensity. Therefore, the β of A and E are larger, leading to that S_4 and σ_φ are also larger than others. When other parameters are almost same (A is compared with B and C, and E is compared with D and F), the larger β causes higher PSLR and more serious image defocusing.

From the form of stripes in Fig.5, it can be seen that the oblique angle of phase screen stripes is related to the propagation angle θ. The ITFs are generated after correction by θ, and the oblique angles of ITF stripes on SAR image are related to the heading of radar beam φ.

For LEO SAR results, it can be seen that $\beta \approx 1$ and the change of drifting velocity has few effects on SAR imaging. Besides, the Δ is much smaller than that of GEO SAR, which causes the better imaging quality.

To sum up, firstly, the angle of platform motion and geomagnetic field will affect the strength of scintillations. The more aligned GEO SAR position with geomagnetic field causes the smaller amplitude scintillation strength and the better the imaging quality. Secondly, the drifting velocity will also affect the strength of scintillations and image quality. The larger β causes the stronger scintillation intensity and the more serious image defocusing. Besides, the oblique angles of light-dark stripes on the SAR image are related to the geometry of satellite and geomagnetic field. Finally, the change of drifting velocity has few effects on LEO SAR imaging and the smaller Δ compared to that of GEO SAR causes the better imaging quality.

V. CONCLUSION

The paper models the effects of drifting anisotropic irregularities on GEO SAR imaging by the modified PSD and analyzes the amplitude and phase fluctuations introduced by ionospheric scintillation through the ITF which is different for various IPP positions. The SAR imaging verification is carried out at 3 selected positions of the big "8" and small "8" GEO SAR, respectively. The geomagnetic field parameters are obtained from IGRF and the velocity and direction of GEO SAR motion are obtained from STK, which are reliable enough to verify the analysis. The simulation results demonstrate that the GEO SAR system is sensitive to the anisotropic and drifting ionospheric irregularities. Firstly, the angle between platform motion and geomagnetic field will

mainly affect the strength of scintillations. The more aligned of two directions causes the smaller amplitude scintillation strength and the better imaging quality. Secondly, the drifting velocity will affect the strength of scintillations and imaging quality. The larger β causes the stronger scintillation intensity and the more serious image defocusing, while the drifting velocity has few effects on LEO SAR. Finally, the oblique angles of light-dark stripes on the SAR image are related to the geometry of satellite and geomagnetic field.

ACKNOWLEDGMENT

The authors thank the geomagnetic field data which is obtained from IGRF: http://wdc.kugi.kyoto-u.ac.jp/igrf/.

REFERENCES

[1] K. C. Yeh and C.-H. Liu, "Radio wave scintillations in the ionosphere," *Proc. IEEE*, vol. 70, no. 4, pp. 324–360, Apr. 1982.
[2] C. S. Carrano, K. M. Groves, and R. G. Caton, "Simulating the impacts of ionospheric scintillation on L band SAR image formation," *Radio Sci.*, vol. 47, no. 4, pp. 1–14, Aug. 2012.
[3] N. C. Rogers and P. S. Cannon, "The synthetic aperture radar transionospheric radio propagation simulator (SAR-TIRPS)," in *Proc. Inst. Eng. Technol. 11th Int. Conf. Ionospheric Radio Syst. Techn. (IRST)*, Apr. 2009, pp. 1–5.
[4] F. J. Meyer, K. Chotoo, S. D. Chotoo, B. D. Huxtable, and C. S. Carrano, "The influence of equatorial scintillation on L-band SAR image quality and phase," *IEEE Trans. Geosci. Remote Sens.*, vol. 54, no. 2, pp. 869–880, Feb. 2016.
[5] J. S. Kim, K. Papathanassiou, H. Sato, and S. Quegan, "Detection and estimation of equatorial spread F scintillations using synthetic aperture radar," *IEEE Trans. Geosci. Remote Sens.*, vol. 55, no. 12, pp. 6713–6725, Dec. 2017.
[6] J. S. Kim, K. P. Papathanassiou, S. Quegan, and N. Rogers, "Estimation and correction of scintillation effects on spaceborne P-band SAR images," in *Proc. IEEE Int. Geosci. Remote Sens. Symp.*, Jul. 2012, pp. 5101–5104.
[7] S. Quegan, J. Green, R. Zandona-Schneider, R. Scheiber, and K. Papathanassiou, "Quantifying and correcting ionospheric effects on P-band SAR images," in *Proc. IGARSS IEEE Int. Geosci. Remote Sens. Symp.*, vol. 2, Jul. 2008, pp. II-541–II-544.
[8] N. Rogers and S. Quegan, "Faraday rotation correction for the ESA BIOMASS P-band synthetic aperture radar," in *Proc. 7th Eur. Conf. Antennas Propag. (EuCAP)*, Apr. 2013, pp. 3919–3923.
[9] A. M. Guarnieri and F. Rocca, "Options for continuous radar Earth observations," *Sci. China Inf. Sci.*, vol. 60, no. 6, p. 060301, 2017.
[10] Y. Ji, Q. Zhang, Y. Zhang, and Z. Dong, "L-band geosynchronous SAR imaging degradations imposed by ionospheric irregularities," *Sci. China Inf. Sci. J.*, vol. 60, no. 6, Jun. 2017, Art. no. 060308.
[11] C. Hu, Y. Li, X. Dong, R. Wang, and D. Ao, "Performance analysis of L-band geosynchronous SAR imaging in the presence of ionospheric scintillation," *IEEE Trans. Geosci. Remote Sens.*, vol. 55, no. 1, pp. 159–172, Jan. 2017.
[12] X. Dong, C. Hu, Y. Tian, W. Tian, Y. Li, and T. Long, "Experimental study of ionospheric impacts on geosynchronous SAR using GPS signals," *IEEE J. Sel. Topics Appl. Earth Observ. Remote Sens.*, vol. 9, no. 6, pp. 2171–2183, Jun. 2016.
[13] S. Mohanty, C. S. Carrano, and G. Singh, "Effect of anisotropy on ionospheric scintillations observed by SAR," *IEEE Trans. Geosci. Remote Sens.*, vol. 57, no. 9, pp. 6888–6899, Sep. 2019.
[14] S. Mohanty and G. Singh, "Improved POLSAR model-based decomposition interpretation under scintillation conditions," *IEEE Trans. Geosci. Remote Sens.*, vol. 57, no. 10, pp. 7567–7578, Oct. 2019.
[15] C. L. Rino, "A power law phase screen model for ionospheric scintillation: 1. Weak scatter," *Radio Sci.*, vol. 14, no. 6, pp. 1135–1145, 1979.
[16] D. L. Knepp, "Multiple phase-screen calculation of the temporal behavior of stochastic waves," *Proc. IEEE*, vol. 71, no. 6, pp. 722–737, Jun. 1983.
[17] J. Wang and Y. T. Morton, "High-latitude ionospheric irregularity drift velocity estimation using spaced GPS receiver carrier phase time–frequency analysis," *IEEE Trans. Geosci. Remote Sens.*, vol. 53, no. 11, pp. 6099–6113, Nov. 2015.

XICHAO DONG received the B.S. degree in electrical engineering and the Ph.D. degree in target detection and recognition from the Beijing Institute of Technology (BIT), Beijing, China, in 2008 and 2014, respectively. From October 2011 to October 2013, he was a Research Assistant with the CTCD, University of Sheffield, Sheffield, U.K. From 2014 to 2017, he held a postdoctoral position with the School of Information and Electronics, BIT, where he became an Associate Professor, in April 2017. His research interests include geosynchronous synthetic aperture radar and weather radar. He was a recipient of the IEEE CIE International Radar Conference Excellent Paper Award, in 2011 and the Chinese Institute of Electronics Youth Conference Poster Award, in 2014

JIAQI HU was born in Henan, China, in 1995. She received the bachelor's degree in information confrontation technology from Xi'dian University, Xi'an, China, in 2017. She is currently pursuing the Ph.D. degree in information and communication engineering with the Beijing Institute of Technology, Beijing, China.

Her main research interests include GEOSAR ionosphere, and tropospheric impact and compensation.

CHENG HU (SM'16) received the B.S. degree in electronic engineering from the National University of Defense Technology, in July 2003, and the Ph.D. degree in target detection and recognition from the Beijing Institute of Technology (BIT), in July 2009. He was a Visiting Research Associate with the University of Birmingham for 15 months, from 2006 to 2007. In September 2009, he joined the School of Information and Electronics, BIT, and has been a Full Professor, since 2014. He is currently the Ph.D. Full Professor/Doctoral Supervisor and the Vice-Director of the Radar Research Lab, BIT. He has published over 60 SCI-indexed journal articles and over 100 conference papers. His main research interests include new concept synthetic aperture radar imaging and the biological detection radar system and signal processing.

YUANHAO LI (M'13) received the B.S. degree in information engineering and the Ph.D. degree in information and communication engineering from the Beijing Institute of Technology (BIT), Beijing, China, in 2012 and 2018, respectively.

From December 2016 to December 2017, he was a Visiting Researcher with the Dipartimento di Elettronica e Informazione, Politecnico di Milano, Milan, Italy. From April 2018 to September 2018, he was a Research Scientist with the Radar Research Laboratory, BIT. Since October 2018, he has been a Postdoctoral Researcher with the Department of Geoscience and Remote Sensing, Delft University of Technology, Delft, The Netherlands. His research interests include SAR system and signal processing, InSAR/D-InSAR technique, ionospheric effects on radar systems, and RFI signal analysis.

Dr. Li is a Reviewer for many international peer-reviewed journals. He was the recipient of the Chinese Institute of Electronics Youth Conference Excellent Paper Award, in 2014.

SHIYU SUN was born in Hunan, China, in 1996. She received the bachelor's degree in electronic information engineering from the Wuhan University of Technology, Wuhan, China, in 2018. She is currently pursuing the master's degree in electronics and communication engineering with the Beijing Institute of Technology (BIT), Beijing, China.

Her main research interests include GEO SAR ionosphere impact and compensation.